ARTICLE IN PRESS – Acta Cryst. B

Acta Cryst B STRUCTURAL SCIENCE CRYSTAL ENGINEERING MATERIALS

ISSN 2052-5206

Synthesis, crystal structure and phase transitions of novel hybrid perovskite: bis(1,2diaminepropane) di-μ-chloro-bis[diaquadichloromanganate(II)] dichloride

Proof instructions

Proof corrections should be returned by **4 July 2023**. After this period, the Editors reserve the right to publish your article with only the Managing Editor's corrections.

Please
(1) Read these proofs and assess whether any corrections are necessary.
(2) Check that any technical editing queries highlighted in **bold underlined** text have been answered.
(3) Send corrections by e-mail to **actab@iucr.org**. Please describe corrections using plain text, where possible, giving the line numbers indicated in the proof. Please do not make corrections to the pdf file electronically and please do not return the pdf file. If no corrections are required please let us know.

To arrange payment for **open access**, please visit **https://scripts.iucr.org/openaccess/?code=yv5010**. To purchase printed offprints, please complete the attached order form and return it by e-mail.

Please check the following details for your article

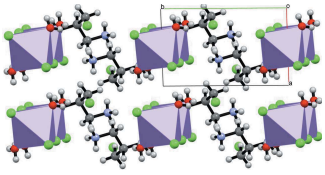

Thumbnail image for contents page

Synopsis: The synthesis and crystal structure of a new hybrid perovskite with manganate(II) for which differential scanning calorimetry (DSC) shows two endothermic main peaks at T = 366 K and T = 375 K are reported. These phase transitions have been investigated using powder diffraction that confirms the presence of a major transition around 363 K in relation with the release of the two **two Mn coordinated water molecules[two water molecules coordinated to Mn?]**.

Abbreviated author list: Abdel-Aal, S.K. (0000-0001-8095-8064); Souhassou, M.; Durand, P.; Lecomte, C.; Abdel-Rahman, A.S. (0000-0003-1910-7011); Claiser, N.

Keywords: lead-free hybrid perovskites; crystal structure; phase transitions; difference scanning calorimetry

How to cite your article in press

Your article has not yet been assigned page numbers, but may be cited using the doi:

Abdel-Aal, S.K., Souhassou, M., Durand, P., Lecomte, C., Abdel-Rahman, A.S. & Claiser, N. (2023). *Acta Cryst.* B**79**, https://doi.org/10.1107/S2052520623005309.

You will be sent the full citation when your article is published and also given instructions on how to download an electronic reprint of your article.

Acta Cryst B
STRUCTURAL SCIENCE
CRYSTAL ENGINEERING
MATERIALS
ISSN 2052-5206

Synthesis, crystal structure and phase transitions of novel hybrid perovskite: bis(1,2diaminepropane) di-μ-chloro-bis[diaquadichloromanganate(II)] dichloride

Seham K. Abdel-Aal,[a]* Mohamed Souhassou,[b] Pierrick Durand,[b] Claude Lecomte,[b] Ahmed S. Abdel-Rahman[a] and Nicolas Claiser[c]*

[a]Physics Department, Faculty of Science, Cairo University, Giza, 12613, Egypt, [b]CNRS, Laboratoire CRM2, UMR CNRS 7036, Université de Lorraine, Boulevard des Aiguillettes, BP 70239, Vandoeuvre-lès-Nancy, 54506, France, and [c]CRM2 (UMR UL-CNRS 7036), Université de Lorraine, Boulevard des Aiguillettes, BP 70239, Vandoeuvre-lès-Nancy, 54506, France. *Correspondence e-mail: seham@sci.cu.edu.eg, nicolas.claiser@univ-lorraine.fr

Received 5 January 2023
Accepted 13 June 2023

Edited by K. E. Knope, Georgetown University, USA

Keywords: lead-free hybrid perovskites; crystal structure; phase transitions; difference scanning calorimetry.

CCDC reference: 2269960

Supporting information: this article has supporting information at journals.iucr.org/b

Single crystals of bis(1,2-diaminepropane) di-μ-chloro-bis[diaquadichloromanganate(II)] dichloride have been prepared by evaporation from ethanoic solution. The triclinic X-ray crystal structure is built as layers of centrosymmetric dimers of $[Mn(Cl)_4,(H_2O)_2]^{2-}$ octahedra and 1,2-diaminepropane. The inorganic part consists of Mn octahedra sharing one edge and distributed in the basal *ac* plane along the *a* direction. These doubly negative charged layers are separated along the *b* axis by a positively charged diamine propane layer. One Cl^- anion contributes to the electroneutrality of the crystal interacting with both inorganic – through a hydrogen bond network to the **two Mn coordinated water molecules[two water molecules coordinated to Mn?]** – and organic layers via the NH_3^+ ammonium group. Differential scanning calorimetry shows two endothermic main peaks at T = 366 K and T = 375 K related to the release of the water molecules. The resulting dehydrated **material is monoclinic C[please clarify wording]** as shown by powder **XRD[X-ray diffraction]**.

1. Introduction

Hybrid organic inorganic perovskites (HOIP) are intensively studied due to their tunable structure and properties. Changing the metal or/and the ligand allows the tuning of optic, electric, magnetic, ferroelectric and multiferroic properties (Jain *et al.*, 2009; Nagabhushana *et al.*, 2015; Gómez-Aguirre *et al.*, 2016; Cortecchia *et al.*, 2019; Zhang *et al.*, 2019). Halide perovskites, in particular lead halides, are interesting semiconductors with a direct band gap (**between 1.5 eV and 2.3 eV** depending on the halide content) which allows the collection of visible photons; they are widely used in photovoltaic applications as solar cells. Recently, the power conversion efficiency based on methyl amine lead iodide reaches over 20% (Park, 2019; Lin, 2020). These luminescent lead-containing crystals have no future for safety and ecological reasons as lead has harmful effects on human health and environment. On the other hand, first row transition metals do not produce interesting luminescence but have interesting multiferroic properties (electric and magnetic) and reversible–irreversible structural phase transitions (Ye *et al.*, 2015; Zhang *et al.*, 2015*a*,*b*; Lv *et al.*, 2016; Mostafa *et al.*, 2017). Among them, manganese halide perovskites crystallized with alkylammonium cations are studied for their potential magnetic properties (Willett & Riedel, 1975; Kind *et al.*, 1978; Ren *et al.*, 2020; Mączka *et al.*, 2020; Neumann *et al.*, 2021) that can be

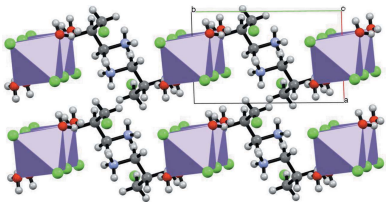

modulated by the **organic ligand and for their interesting phase diagrams due to the frustration of the NH_3^+ group to interact with Cl^- ions to form ammonium chloride hydrogen bonds [please make wording clearer]** (Depmeier, 2009).

A_2MX_4 type aliphatic hybrid perovskites refer to 2D hybrid perovskites where **[charges needed on cation/anions->]** A is an **ammonium organic cation[alkylammonium cation]** of selected chain length, M^{2+} is a divalent cation (Co, Cu, Mn, ...) and X^- is a halogen anion (Cl, Br). Hybrid perovskites containing ammonium groups at the end of the aliphatic chain usually refer to diammonium hybrid perovskites [NH_3-$(CH_2)_n$-NH_3)MX_4] (Park, 2019; Lin, 2020; Mondal *et al.*, 2017; Abdel-Aal, 2017; Cortecchia *et al.*, 2017; Abdel-Aal & Ouasri, 2022; Abdel-Aal *et al.*, 2022). Crystal structure and physico-chemical properties depend on the characteristics of organic cations and inorganic anions. Layered diammonium hybrid Mn halide perovskites consist of $(MX_6)^{2-}$ octahedra separated by a diammonium organic monolayer. The cavities between the octahedra are occupied by the organic ligands interacting via N—H$\cdots X$ hydrogen bonds with the **octahedron[octahderal] halides** (Mondal *et al.*, 2017; Abdel-Aal *et al.*, 2022).

In the present paper the crystal structure and phase transitions of a novel Mn hybrid perovskite is described: bis(1,2-diamine propane) di-μ-chloro-bis[diaquadichloromanganate (II)] dichloride (compound **1)**.

2. Experimental

2.1. Synthesis

The chemicals used are from SIGMA-ALDRICH with purity exceeding 99%. Solvents were of reagent grade. Diamino **propan-chloride[?]** $[NH_3CH_2CH(NH_3)CH_3]Cl_2$ was synthesized by adding drop by drop 30% HCl to 1,2-di-aminopropane (4 mg) dissolved in ethanol solution (100 ml) and placed in an ice bath until pH $\sim$ 4. The resulting solution was heated up to **60°C[333 K]** for 30 min under constant stirring. Colorless needle crystals of $[NH_3CH_2CH(NH_3)CH_3]Cl_2$ precipitated out upon gradual cooling to room temperature. The crystals were filtered, dried and kept in a vacuum desiccator until use.

Perovskite hybrid crystals of **$[NH_3CH_2CH(NH_3)CH_3]$ Cl $MnCl_3.2H_2O$ [spacing round Cl?]** were prepared by mixing 1 M of ethanolic solution of both $[NH_3CH_2CH(NH_3)CH_3]Cl_2$ and $MnCl_2.4H_2O$ in 1:1 stoichiometric ratio (organic/inorganic), under constant stirring, then heated up to **60°C[333 K]** for 30 min followed by slow cooling to room temperature in a double-wall container. Pink needle crystals of (**1**) precipitated out. The reaction proceeds according to the following scheme:

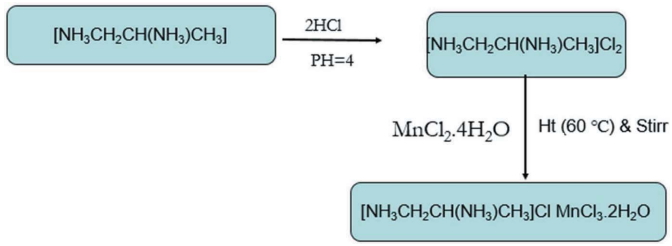

Good quality crystals were selected for single crystal and powder X-ray diffraction measurements.

2.2. Differential scanning calorimetry DSC

Thermal characteristics of **1** in the 300–474 K temperature range were studied on a Shimadzu-60 differential thermal scanner at a scanning speed of 10 K min^{-1}. The analyzer was calibrated with the melting transition of indium at 430 K. Measurements were performed in a flow of nitrogen gas. A first heating run was performed on **1**, then the resulting material was cooled down before a second heating run.

2.3. X-ray powder diffraction.

Powder XRD data were measured with a Panalytical X'Pert Pro MPD diffractometer equipped with X'celerator detector, variable temperature and monochromated Cu $K\alpha1$ radiation. Measurements from room temperature to 523 K in 10 K step were performed (22 points measured, 90 min per point). A more precise measurement at room temperature was carried out on a powder heated overnight at 373 K (22 h measurement). The obtained cell is C-centered monoclinic as found with the **DICVOL indexing algorithm [lieterature ref needed?]**: out of 45 peaks used, 34 peaks were single indexed and **0[no]** peaks were unindexed with a tolerance of 0.03° in 2θ angle leading to a very good figure of merit [F(30) = 139.9].

2.4. Single crystal XRD and structure refinement

A single crystal of **1** was selected and X-ray diffraction intensities were measured on a **Rigaku Oxford Diffraction** SuperNova dual Mo/Cu Atlas diffractometer. The **parallele-piped [called needles earlier on!]** crystal was kept at 100 (5) K during data collection. Absorption correction was made using *Abspack* and all 29228 collected reflections **were merged in** 6040 independent ones **($I > 0$)** using *CrysAlis* software (Rigaku Oxford Diffraction, 2020) with an agreement R_{int} = 0.060. The structure was solved using *Olex2* (Dolomanov *et al.*, 2009) by deconvolution of Patterson peaks and refined using a Gauss–Newton minimization (Bourhis *et al.*, 2015). All details about the data collection and refinement statistics **for 1** are given in Table 1.

3. Results and discussion

3.1. Crystal structure description

The crystal structure of **1**, Fig. 1, can be described as layers of doubly negative charged centrosymmetric dimers of

Table 1
Experimental details **for 1**.

Crystal data	
Chemical formula	$Cl_3H_4MnO_2{\cdot}C_3H_{12}N_2{\cdot}Cl$
M_r	308.92
Crystal system, space group	Triclinic, $P\overline{1}$
Temperature (K)	100
a, b, c (Å)	5.9138 (2), 9.8318 (4), 10.8908 (4)
α, β, γ (°)	73.154 (4), 76.691 (3), 87.551 (3)
V (Å^3)	589.58 (4)
Z	2
Radiation type	Mo $K\alpha$
μ (mm^{-1})	2.00
Crystal size (mm)	**× _ × ??**
Data collection	
Diffractometer	?
Absorption correction	?
No. of measured, independent and observed [$I \geq 2u(I)$] reflections	29228, 6040, 4678
R_{int}	0.060
$(\sin\theta/\lambda)_{max}$ (Å^{-1})	0.859
Refinement	
$R[F^2 > 2\sigma(F^2)]$, $wR(F^2)$, S	0.033, 0.074, 1.00
No. of reflections	6040
No. of parameters	128
H-atom treatment	H atoms treated by a mixture of independent and constrained refinement
$\Delta\rho_{max}$, $\Delta\rho_{min}$ (e Å^{-3})	0.90, −0.88

Computer programs: *SHELXS* (Sheldrick, 2008), *OLEX2.refine* (Bourhis *et al.*, 2015), *OLEX2* (Dolomanov *et al.*, 2009).

$[Mn(Cl)_4,(H_2O)_2]^{2-}$ octahedra sharing one edge and distributed in the basal *ac* plane along the *a* direction. The manganese Mn^{2+} cations are μ-coordinated by Cl^- anions in the basal plane and by two waters molecules in axial position [Mn–Mn = 3.7536 (2) Å]. These Mn dimers are connected along the *a* axis via two Cl···H—O interactions and sandwiched along the *b* axis by the doubly positive diamine propane layer ($2NH_3^+$ moieties per molecule).

The **supplemental[additional]** Cl^- anion (Cl4) ensures the electroneutrality of the crystal and stabilizes the crystal structure through interactions with the inorganic part via two Cl4···H—O halogen bonds (to the two Mn coordinated water molecules) and the $N_1H_3^+$ ammonium group (Table 2). The Mn coordinated chlorine atoms form six **supplementary** Cl···H—N halogen bond that tie the inorganic and organic layers together along the *b* direction (the average Cl···H bond distance is 2.57 Å).

The Mn—μCl distances are almost equal (2.55 **(X)** Å)**[It is not clear which bonds this distance refers to, and Mn-Cl distances are not equivalent within s.u. limits.]** with a bridging Mn—Cl—Mn angle of 94.72 (1)°. This latter value is identical to those observed in similar dimers: 94.57 **(X)**° in isopropylammonium trichloromanganate(II) dihydrate (**2**) (Willett, 1979) or 94.55 **(X)**° and 94.41 **(X)**° reported by Dörhöfer & Depmeier (1979) and Jin *et al.* (2005)**, respectively[?]**. In **1** the terminal Mn—Cl distances are different: Mn—Cl1 = 2.4735 (4) Å and Mn—Cl3 = 2.5660 (4) Å. The axial water molecules distances differ by 0.05 Å, Mn—O2 = 2.213 (1) and Mn—O1 = 2.160 (1) Å with an O1—Mn—O2 angle of 177.51 (4)°. The Mn atom is 0.031 **(X)** Å out of **the plane of** the four equatorial Cl atoms, 0.020 **(X)** Å out of the plane formed by Cl1, Cl2 and the two water O atoms, and 0.051 **(X)** Å out of the plane formed by Cl2 and Cl3 and the two water O atoms. The following **DI[what does DI**

Table 2
List of the shortest cation–anion interactions**[Why are these not (also) referred to as hydrogen bonds?]** in **1**.

Cl4 is not coordinated to Mn. **Ho - holmium[!], so changed to Hw (here and cif)**

D—H···A (Å)	D—H (Å)	H···A (Å)	D···A (Å)	D —H···A (°)
N2—H2A···Cl1	0.910 (7)	2.559 (10)	3.2710 (13)	135.5 (6)
N2—H2B···Cl1	0.910 (4)	2.372 (4)	3.1881 (13)	149.2 (7)
N2—H2B···Cl1	0.910 (4)	2.735 (8)	3.1899 (12)	112.0 (5)
O2—**Hw**2B···Cl2	0.77 (2)	2.49 (2)	3.1986(11)	154 (3)
O1—**Hw**1B...Cl3	0.83 (2)	2.33 (2)	3.1382 (12)	164 (2)
N2—H2C···Cl3	0.911 (6)	2.378 (6)	3.2788 (12)	170.0 (4)
N1—H1A···Cl3	0.910 (4)	2.394 (3)	3.3031 (13)	177.1 (7)
N2—H2A···O2	0.910 (7)	2.238 (4)	2.9701 (16)	137.1 (7)
N1—H1B···Cl4	0.910 (6)	2.376 (6)	3.2213 (12)	154.6 (5)
N1—H1C···Cl4	0.910 (7)	2.307 (7)	3.1775 (12)	160.0 (6)
O2—**Hw**2A···Cl4	0.82 (3)	2.29 (3)	3.0963 (12)	167 (2)
O1—**Hw**1A···Cl4	0.76 (3)	2.37 (3)	3.1167 (13)	168 (2)

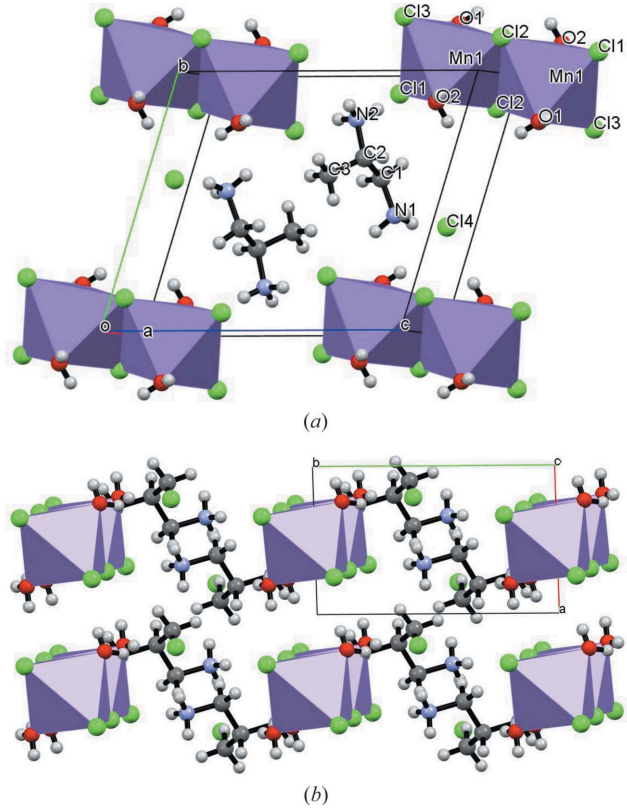

Figure 1
3D view of the structure of **1** at 100 K (*a*) along the *a* axis and (*b*) along the *a* axis. **[please provide replacement Fig. 1a without labels overlapping atoms]**

Table 3
Bond lengths (Å) and angles (°) for **1**.

Mn1—Cl1	2.4735 (4)	Mn1—O2	2.213 (1)
Mn1—Cl2	2.5392 (4)	N1—C1	1.491 (2)
Mn1—Cl21	2.5634 (4)	C2—C1	1.526 (2)
Mn1—Cl3	2.5660 (4)	C2—C3	1.524 (2)
Mn1—O1	2.160 (1)	N2—C2	1.496 (2)
Cl3—Mn1—Cl2	90.619 (12	O2—Mn1—Cl2	89.52 (3)
Cl3—Mn1—Cl2^{i}	175.883 (12)	O2—Mn1—Cl2^{i}	90.25 (3)
Cl1—Mn1—Cl2	175.328 (14)	O2—Mn1—Cl3	89.34 (3)
Cl1—Mn1—Cl2^{i}	90.686 (12)	O2—Mn1—Cl1	88.14 (3)
Cl1—Mn1—Cl3	93.395 (12)	O2—Mn1—O1	177.51 (5)
O1—Mn1—Cl2	90.07 (3)	C1—C2—N2	107.32 (11)
O1—Mn1—Cl2^{i}	92.17 (3)	C3—C2—N2	108.63 (11)
O1—Mn1—Cl3	88.20 (3)	C3—C2—C1	114.11 (11)
O1—Mn1—Cl1	92.44 (3)	C2—C1—N1	111.01 (11)
Cl2—Mn1—Cl2^{i}	**85.28 (1)**		

Symmetry code: (i) $1-x, 2-y, -z$.

mean?](related to the distances) and **DA[is this not confusing? donor-acceptor?]**(based on the angles) indices [equations (1) and (2) (Baur, 1974)] characterize the [$MnCl_4$-[·]$2H_2O$] octahedron's distortion

$$\mathrm{DI} = \frac{1}{nD_{\mathrm{avg}}} \sum_{i=1}^{n} \left|D_i - D_{\mathrm{avg}}\right|, n = 6 \quad (1)$$

$$\mathrm{DA} = \frac{1}{mA_{\mathrm{avg}}} \sum_{j=1}^{m} \left|A_i - A_{\mathrm{avg}}\right|, m = 12 \quad (2)$$

where A_{avg} and D_{avg} are the mean values of the octahedron angles and distances, respectively. The DI and DA distortions for Mn are 6.4% and 1.8%, respectively, indicating a small distortion mostly due to the apical water molecules as DI (Mn—Cl) is only 1.2%. In comparison, DI and DA distortions for Mn in **2** are 3.7%, and 2.4%, respectively, indicating a that the distortion induced by the apical water molecules is smaller in this case [DI(Mn—Cl) is 1.8% in **2**]).

A consultation of the Cambridge Crystallographic Data Centre (CCDC) (**Groom *et al.*, 2016**) indicates five other crystal structures with similar Mn octahedron dimers coordinated **to[with]** four or five chlorine anions and one or two water molecules (Willett, 1979; Dörhöfer & Depmeier, 1979; Jin *et al.*, 2005; Baur, 1974; Prince *et al.*, 2003; Lee *et al.*, 2003), some with different conformations depending on the axial position or not of the water molecule(s). Only one dimer (**2**),

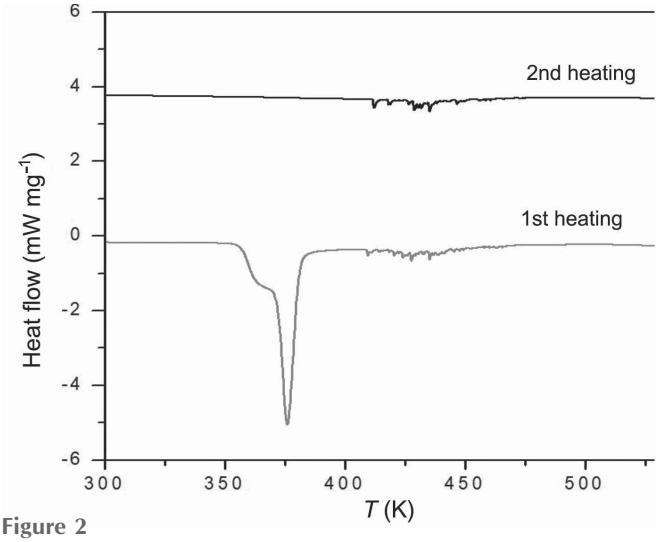

Figure 2
Thermograph of **1** for first heating and second heating (upper graph, **deported[?]**). **[Please reword whole caption]**

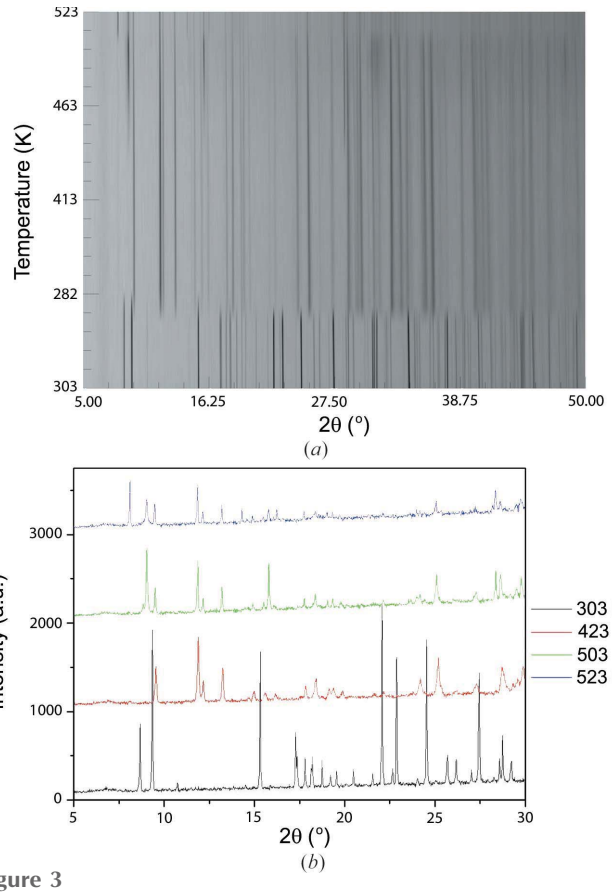

Figure 3
Powder XRD as function of temperature and 2θ **of 1?**: (*a*) **top-full** diffraction pattern, (*b*) diffraction patterns at 303, **403[423?]**, 503 and 523 K.

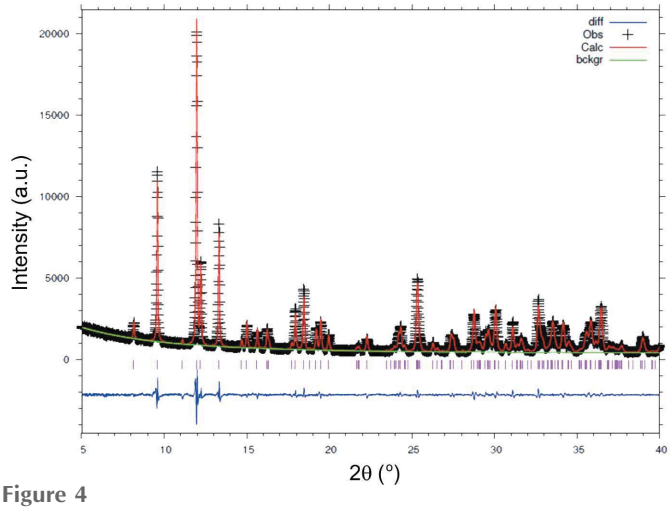

Figure 4
Room-temperature powder XRD pattern **of 1?]**after heating at 373 K and corresponding Le Bail extraction.

see above, has the same conformation as **1** with similar Mn_{axial}–H_2O and $Mn_{terminal}$–Cl distances and an Mn—Cl—Mn bridge angle of 94.57°. Among all these Mn dimers only bis(piperazinium) di-μ-chloro-bis[diaquadichloromanganate(II)] dichloride crystal (Jin *et al.*, 2005) contains an isolated Cl anion which ensures electroneutrality and crystal stability; this isolated Cl^- is also involved in eight Cl···H contacts, four of them are Cl···H—O connecting Mn octahedral dimers. The conformation of these octahedra differs from **1** with at least one water molecule in the basal plane. **Table 3 not called out/referred to in text**

3.2. Analysis of the phase transformations versus temperature

Organic–inorganic hybrid perovskites usually present thermal phase transitions (Mikhail, 1977; Tichý *et al.*, 1980; Crowley *et al.*, 1982) but to the best of our knowledge, no structural phase transition has been previously characterized for $(MnCl_5H_2O)^{2-}$ and $[MnCl_4(H_2O)_2]^F$ structures. DSC and variable X-ray powder diffraction have been performed between room temperature and 523 K in 10 K steps.

The DSC thermograph shows five endothermic peaks (**Fig. 2**): T_1 at 366 K (ΔH = 35 J g^{-1}), T_2 at 375 K (ΔH = 48 J g^{-1}), T_3 at 416 K (ΔH = 1.15 J g^{-1}), T_4 at 425 K (152°C, ΔH = 1.57 J g^{-1}) and T_5 at 416 K (163°C, ΔH = 2.19 J g^{-1}). **1** undergoes two continuous phase changes at 366 K and 375 K, respectively. These changes originate from the release of the water molecules: for the first water molecule the onset temperature is 343 K, ending at 371 K. The second endothermic peak (T = 375 K) with a 'λ' shape starts at 370 K and ends at 383 K. **[It is unclear whether the sample has been left exposed to air, and for how long, to check for irreversibility.]** After cooling down, the same powder is warmed again. The second heating curve does not present any significant event before 400 K indicating that the transformations related to T_1 and T_2 are irreversible.

These thermodynamic data agree with the variable temperature powder X-ray diffraction pattern (**Fig. 3**) and confirm the existence of phase transformations. The first transition occurs around 353 K in accordance with the DSC measurements (due to the removal of the Mn coordinated water molecules). **[Are you trying to say that the phases coexist of a range of 15 K? If so, this is not at all clear.]**The two phases coexist within almost **15°C[288 K]**, which means that some crystallites undergo the phase transition, while others are still in the low-temperature phase. The first (low-order) reflection, **which[whose] intensity strongly depends on** the water molecules of **1**, disappears at 363 K strengthening the hypothesis that this transition is due to the loss of water molecules[1]. Three other structural changes are observed: around 443 K, 493 K and 513 K.

Fresh powder of **1** was left overnight under air in an oven at at 373 K. Powder X-ray diffraction measurement was then performed at room temperature on the resulting powder. The diffractogram shows the absence of the starting product (hydrated phase). The good quality of these data allowed us to apply the DICVOL indexing algorithm that matched on a *C*-centered monoclinic cell with a = 15.676 (3) Å, b = 15.959 (3) Å, c = 12.769 (3) Å, β = 109.03 (1)° and V = 3020 (2) Å^3 (Table S1) and then a Le Bail extraction was performed using this unit cell (Fig. 4). This new dehydrated phase is not simply related to the structure of **1** as the diffraction patterns are completely different. Further work to solve the dehydrated structure is underway.

[1] We calculated the simulated powder XRD patterns for (1) at room temperature with and without O1, O2 and Cl4 contributions. The more visible difference is the disappearance of the first observed reflection from the second spectra (see supplementary materials Fig. S1 and S2).

4. Conclusion

Single crystals of a novel hybrid perovskite **[$NH_3CH_2CH(NH_3)CH_3$]ClMnCl$_3$**·2H_2O, bis(1,2-diaminepropane) di-μ-chloro-bis[diaquadichloromanganate(II)] dichloride were successfully prepared **[clarification of meaning needed]by evaporation and gradual cool method from 333 K to room temperature**. The X-ray structure shows layers of centrosymmetric dimers of $[Mn(Cl)_4,(H_2O)_2]^{2-}$ octahedra sharing one edge and distributed in the basal *ac* plane along the *a* direction. Hydrogen bonds connect the organic to the inorganic parts and ensure **the stability of an[the] isolated chlorine[chloride] ion.[unclear, please check meaning]** DSC and variable temperatures powder X-ray diffraction experiments indicate an irreversible phase transition from triclinic phase at room temperature to a *C*-centered monoclinic phase at 373 K. First-row transition metals HOIP have interesting reversible irreversible structural phase transitions. Since in cited compounds (Ye *et al.*, 2015; Zhang *et al.*, 2015*a*,*b*; Mostafa *et al.*, 2017), the $(MX_6)^{2-}$ metal octahedra differ from that of **1**, therefore, the observed structural phase transition is unprecedented as related to the loss of coordinated water. Furthermore, to the best of our knowledge, no structural phase transition has been previously characterized for related $(MnCl_5H_2O)^{2-}$ and $[MnCl_4(H_2O)_2]^F$ structures (Willett, 1979; Dörhöfer & Depmeier, 1979; Jin *et al.*, 2005; Baur, 1974; Prince *et al.*, 2003; Lee *et al.*, 2003) thus we plan to further explore them.

Acknowledgements

We acknowledge access to the PMD^{2}X X-ray diffraction facility of the CRM2 laboratory, CNRS-Université de Lorraine, France.

References

Abdel-Aal, S. K. (2017). *Solid State Ionics*, **303**, 29–36.
Abdel-Aal, S. K., Bortel, G., Pekker, Á., Kamarás, K., Faigel, G. & Abdel-Rahman, A. S. (2022). *J. Phys. Chem. Solids*, **161**, 110400.
Abdel-Aal, S. K. & Ouasri, A. (2022). *J. Solid State Chem.* **314**, 123401.
Baur, W. H. (1974). *Acta Cryst.* B**30**, 1195–1215.
Bourhis, L. J., Dolomanov, O. V., Gildea, R. J., Howard, J. A. K. & Puschmann, H. (2015). *Acta Cryst.* A**71**, 59–75.
Cortecchia, D., Mróz, W., Neutzner, S., Borzda, T., Folpini, G., Brescia, R. & Petrozza, A. (2019). *Chem*, **5**, 2146–2158.

Cortecchia, D., Soci, C., Cametti, M., Petrozza, A. & Martí-Rujas, J. (2017). *ChemPlusChem*, **82**, 681–685.

Crowley, J. C., Dodgen, H. W. & Willett, R. D. (1982). *J. Phys. Chem.* **86**, 4046–4055.

Depmeier, W. (2009). *Cryst. Res. Technol.* **44**, 1122–1130.

Dolomanov, O. V., Bourhis, L. J., Gildea, R. J., Howard, J. A. K. & Puschmann, H. (2009). *J. Appl. Cryst.* **42**, 339–341.

Dörhöfer, K. & Depmeier, W. (1979). *Z. Anorg. Allg. Chem.* **448**, 181–187.

Gómez-Aguirre, L. C., Pato-Doldán, B., Stroppa, A., Yang, L.-M., Frauenheim, T., Mira, J., Yáñez-Vilar, S., Artiaga, R., Castro-García, S., Sánchez-Andújar, M. & Señarís-Rodríguez, M. A. (2016). *Chem. Eur. J.* **22**, 7863–7870.

Groom, C. R., Bruno, I. J., Lightfoot, M. P. & Ward, S. C. (2016). *Acta Cryst.* B**72**, 171–179.

Jain, P., Ramachandran, V., Clark, R. J., Zhou, H. D., Toby, B. H., Dalal, N. S., Kroto, H. W. & Cheetham, A. K. (2009). *J. Am. Chem. Soc.* **131**, 13625–13627.

Jin, Z.-M., Li, L., Li, M.-C., Hu, M.-L. & Shen, L. (2005). *Acta Cryst.* E**61**, m1711–m1713.

Kind, R., Plesko, S. & Roos, J. (1978). *Phys. Status Solidi A*, **47**, 233–240.

Lee, J. P., Lewis, B. D., Mendes, J. M., Turnbull, M. M. & Awwadi, F. F. (2003). *J. Coord. Chem.* **56**, 1425–1442.

Lin, C. (2020). *Front. Chem.* **8**, 592.

Lv, X.-H., Liao, W.-Q., Li, P.-F., Wang, Z.-X., Mao, C.-Y. & Zhang, Y. (2016). *J. Mater. Chem. C*, **4**, 1881–1885.

Mączka, M., Gągor, A., Pikul, A. & Stefańska, D. (2020). *RSC Adv.* **10**, 19020–19026.

Mikhail, I. (1977). *Acta Cryst.* B**33**, 1317–1321.

Mondal, P., Abdel-Aal, S. K., Das, D. & Islam, S. M. (2017). *Catal. Lett.* **147**, 2332–2339.

Mostafa, M. F., Elkhiyami, S. S. & Alal, S. A. (2017). *Mater. Chem. Phys.* **199**, 454–463.

Nagabhushana, G. P., Shivaramaiah, R. & Navrotsky, A. (2015). *J. Am. Chem. Soc.* **137**, 10351–10356.

Neumann, T., Feldmann, S., Moser, P., Delhomme, A., Zerhoch, J., van de Goor, T., Wang, S., Dyksik, M., Winkler, T., Finley, J. J., Plochocka, P., Brandt, M. S., Faugeras, C., Stier, A. V. & Deschler, F. (2021). *Nat. Commun.* **12**, 3489.

Park, N.-G. (2019). *ACS Energy Lett.* **4**, 2983–2985.

Prince, B. J., Turnbull, M. M. & Willett, R. D. (2003). CSD Communication: CCDC Number 175501.

Ren, L., Wang, Y., Wang, M., Wang, S., Zhao, Y., Cazorla, C., Chen, C., Wu, T. & Jin, K. (2020). *J. Phys. Chem. Lett.* **11**, 2577–2584.

Rigaku Oxford Diffraction (2020). *CrysAlisPro Software system*, version 1.171.41-64.93a. Rigaku Corporation, Wroclaw, Poland.

Sheldrick, G. M. (2008). *Acta Cryst.* A**64**, 112–122.

Tichý, K., Beneš, J., Kind, R. & Arend, H. (1980). *Acta Cryst.* B**36**, 1355–1367.

Willett, R. D. (1979). *Acta Cryst.* B**35**, 178–181.

Willett, R. D. & Riedel, E. F. (1975). *Chem. Phys.* **8**, 112–122.

Ye, H.-Y., Zhou, Q. H., Niu, X. H., Liao, W. Q., Fu, D.-W., Zhang, Y., You, Y.-M., Wang, J. L., Chen, Z.-N. & Xiong, R.-G. (2015). *J. Am. Chem. Soc.* **137**, 13148–13154.

Zhang, Y., Liao, W.-Q., Fu, D.-W., Ye, H.-Y., Chen, Z.-N. & Xiong, R.-G. (2015*b*). *J. Am. Chem. Soc.* **137**, 4928–4931.

Zhang, Y., Liao, W.-Q., Fu, D.-W., Ye, H. Y., Liu, C. M., Chen, Z.-N. & Xiong, R.-G. (2015*a*). *Adv. Mater.* **27**, 3942–3946.

Zhang, Z., Tang, H., Cheng, D., Zhang, J., Chen, Y., Shen, X. & Yu, H. (2019). *Results Phys.* **12**, 2183–2188.

Acta Cryst B
STRUCTURAL SCIENCE
CRYSTAL ENGINEERING
MATERIALS

ISSN: 2052-5206

ORDER FORM

YOU WILL AUTOMATICALLY BE SENT DETAILS OF HOW TO DOWNLOAD AN ELECTRONIC REPRINT OF YOUR PAPER, FREE OF CHARGE. PRINTED REPRINTS MAY BE PURCHASED USING THIS FORM.

Please scan your order and send to ab@iucr.org

INTERNATIONAL UNION OF CRYSTALLOGRAPHY
5 Abbey Square
Chester CH1 2HU, England.

VAT No. GB 161 9034 76

Article No.: B230530-YV5010

Title of article Synthesis, crystal structure and phase transitions of novel hybrid perovskite: bis(1,2diaminepropane) di-μ-chloro-bis[diaquadichloromanganate(II)] dichloride

Name Nicolas Claiser

Address CRM2(UMR UL-CNRS 7036), Université de Lorraine, Faculté des Sciences et Technologies, Université de Lorraine BP 70239, Boulevard des Aiguillettes, Vandoeuvre-lŁs-Nancy, 54506 , France

E-mail address (for electronic reprints) nicolas.claiser@univ-lorraine.fr

OPEN ACCESS

IUCr journals offer authors the chance to make their articles open access on **Crystallography Journals Online**. If you wish to make your article open access please go to https://scripts.iucr.org/openaccess/?code=YV5010

The charge for making an article open access is from **1800 United States dollars** (for full details see https://journals.iucr.org/b/services/openaccess.html). For authors in European Union countries, VAT will be added to the open-access charge.

DIGITAL PRINTED REPRINTS

I wish to order . . . . . paid reprints

These reprints will be sent to the address given above. If the above address or e-mail address is not correct, please indicate an alternative:

PAYMENT (REPRINTS ONLY)

Charge for reprints . . . . . USD

☐ An official purchase order made out to **INTERNATIONAL UNION OF CRYSTALLOGRAPHY** ☐ is enclosed ☐ will follow

Purchase order No.

☐ Please invoice me

☐ I wish to pay by credit card

EU authors only: VAT No:

Date | Signature

OPEN ACCESS

The charge for making an article open access is from **1750 United States dollars** (for full details see https://journals.iucr.org/b/services/openaccess.html). For authors in European Union countries, VAT will be added to the open-access charge.

DIGITAL PRINTED REPRINTS

An electronic reprint is supplied free of charge.

Printed reprints without limit of number may be purchased at the prices given in the table below. The requirements of all joint authors, if any, and of their laboratories should be included in a single order, specifically ordered on the form overleaf. All orders for reprints must be submitted promptly.

Prices for reprints are given below in **United States dollars** and include postage.

	Size of paper (in printed pages)				
Number of reprints required	1–2	3–4	5–8	9–16	Additional 8's
50	184	268	372	560	246
100	278	402	556	842	370
150	368	534	740	1122	490
200	456	664	920	1400	610
Additional 50's	86	128	178	276	116

PAYMENT AND ORDERING

Official purchase orders should be made out to **INTERNATIONAL UNION OF CRYSTALLOGRAPHY**.

Orders should be returned by email to ab@iucr.org

ENQUIRIES

Enquiries concerning reprints should be sent to support@iucr.org.